

# Atomic clusters submitted to an intense short laser pulse: A density-functional approach

Valérie Vénier, Richard Taïeb, and Alfred Maquet

*Laboratoire de Chimie Physique-Matière et Rayonnement, Université Pierre et Marie Curie,  
11, Rue Pierre et Marie Curie, 75231 Paris Cedex 05, France*

(Received 23 May 2001; published 11 December 2001)

We report the results of a theoretical study of the response of atomic clusters to an intense short laser pulse. Numerical simulations are based on a time-dependent density-functional method for a one-dimensional model of chain of atoms. The electron dynamics is investigated with frozen ion positions. Results concerning the initial stage of ionization, together with high-order harmonic generation are presented.

DOI: 10.1103/PhysRevA.65.013202

PACS number(s): 36.40.-c, 42.65.Ky, 32.80.Rm

## I. INTRODUCTION

Recent experiments have shown that clusters, irradiated by a strong laser pulse, can display a behavior significantly different from the behavior of atoms or molecules: generation of highly charged ions and electrons emitted with very high kinetic energies and emission of intense incoherent x-ray radiation [1,2]. It was also shown that rare-gas clusters can emit high-order harmonics with a significantly higher efficiency than that produced from atomic samples with the same density [3,4]. It was found that, in some cases, a five-fold enhancement of the number of emitted photons could be expected from clusters. Moreover, the dependence of the harmonic yield on the backing pressure was measured, showing an anomalous  $p^3$  scaling law instead of the usual  $p^2$  law observed in monomer gases.

Hot electrons, hard x rays, and highly charged ions are produced at higher intensities, typically  $I_L > 10^{16}$  W/cm<sup>2</sup>. These effects come from the response of the underdense plasma created after the atoms in the clusters have been stripped from their outer electrons. On the other hand, harmonic generation is observed at much lower intensities, namely, around  $I_L \approx 10^{14}$  W/cm<sup>2</sup>. In the following, we will restrict ourselves to this moderate intensity regime and we will concentrate on harmonic generation in a linearly polarized field and on the early stage of atomic ionization within the cluster.

Previous theoretical efforts concerning the interaction of an intense laser field with complex systems such as molecules or molecular ions have shown new phenomena including enhanced ionization, [5–7] and the possibility of increasing the order of generated harmonics, [8–10]. Multiwell potentials have been widely used to model molecular ions [9] ionized clusters, [11] chains of atoms, [12] or model of metals, [13] and most of these studies were restricted to the case of the so-called single-active electron approximation. To our knowledge, in this framework, the only quantum calculation for many-electron neutral systems has been devoted to the  $H_2$  or  $H_3^+$  case, [7,14,15] and a fully correlated, three-dimensional calculation for large neutral systems, such as atomic clusters, seems barely tractable.

Regarding rare-gas clusters irradiated by strong laser fields, the first theoretical calculations have mainly dealt with the production of highly charged ions and also with the charged particle dynamics, see for instance, [16,17] for a

classical Monte Carlo approach or [18] for a Thomas-Fermi model. However, a first attempt to discuss harmonic generation in atomic clusters was presented in [19], through a simplified model. It is the aim of this paper to investigate theoretically the electron dynamics of rare-gas clusters in the moderate intensity regime, beyond the single-active electron approximation. The theoretical tool is based on the time-dependent density-functional theory (TDDFT), which allows, in principle, to incorporate correlation effects due to electron-electron interaction.

The organization of the paper is as follows: in Sec. II, we shall present the theoretical background. Numerical results concerning the ionization of rare-gas clusters will be presented in Sec. III, while harmonic generation will be discussed in Sec. IV. A brief conclusion will end the paper in Sec. V.

## II. THEORETICAL BACKGROUND

The advantage of the density-functional theory is that it allows a many-particle problem to be transformed into a single-particle problem in an—in principle—exact way. According to the theorem of Runge and Gross [20], in a time-dependent problem, every observable can be obtained from the time-dependent density, defined as

$$\rho(\mathbf{r}, t) = \sum_{i=1}^n |\phi_i(\mathbf{r}, t)|^2, \quad (1)$$

where  $n$  is the number of electrons in the system. Atomic units are used throughout, except otherwise stated. The orbital  $\phi_i$  satisfies the time-dependent Kohn-Sham equation

$$i \frac{\partial}{\partial t} \phi_i(\mathbf{r}, t) = \left[ -\frac{\Delta^2}{2} + V_{ext}(\mathbf{r}, t) + \int d^3\mathbf{r}' \frac{\rho(\mathbf{r}', t)}{|\mathbf{r} - \mathbf{r}'|} + V_{xc}[\rho](\mathbf{r}, t) \right] \phi_i(\mathbf{r}, t), \quad (2)$$

where the potential  $V_{ext}$  is given by:

$$V_{ext}(\mathbf{r}, t) = \mathbf{E}(t) \cdot \mathbf{r} - \sum_{j=1}^N \frac{Z}{|\mathbf{r} - \mathbf{R}_j|}. \quad (3)$$

$V_{ext}$  contains two parts: one is the time-dependent coupling with the electric field  $\mathbf{E}(t)$  of the laser, while the other is the static Coulomb interaction with the nuclei.  $N$  represents the number of atoms in the cluster, the  $j$ th nucleus, with charge  $Z$ , being located at the position  $\mathbf{R}_j$ .

The exchange-correlation potential is a functional of the time-dependent density  $\rho$  and, in practice, has to be approximated. In the following, we will use a time-dependent scheme, based on the so-called optimized potential method for spin-polarized systems. In this approach, known as the KLI method, originally proposed by Krieger, Li, and Iafrate [21] and extended into the time-dependent domain [22,23], the exchange-correlation potential  $V_{xc}^{KLI}$  is expressed as explicit functionals of the orbitals  $\phi_{j\sigma}$ , where  $\sigma$  stands for the spin of the electrons. In the exchange-only case, if correlation effects are neglected, the potential reads

$$V_{x\sigma}^{KLI}(\mathbf{r},t) = w_{x\sigma}(\mathbf{r},t) + \frac{1}{\rho_{\sigma}(\mathbf{r},t)} \sum_j^{n_{\sigma}} \rho_{j\sigma}(\mathbf{r},t) \times \int d^3r' \rho(\mathbf{r}',t) V_{x\sigma}^{KLI}(\mathbf{r}',t) \quad (4)$$

with

$$w_{x\sigma}(\mathbf{r},t) = -\frac{1}{\rho_{\sigma}(\mathbf{r},t)} \sum_{j,k}^{n_{\sigma}} \left[ \phi_{j\sigma}(\mathbf{r},t) \phi_{k\sigma}^*(\mathbf{r},t) \int d^3r' \times \frac{\phi_{k\sigma}(\mathbf{r}',t) \phi_{j\sigma}^*(\mathbf{r}',t)}{|\mathbf{r}-\mathbf{r}'|} - \rho_{j\sigma}(\mathbf{r},t) \int d^3r'' \int d^3r' \times \frac{\phi_{j\sigma}(\mathbf{r}'',t) \phi_{k\sigma}^*(\mathbf{r}'',t) \phi_{k\sigma}(\mathbf{r}',t) \phi_{j\sigma}^*(\mathbf{r}',t)}{|\mathbf{r}''-\mathbf{r}'|} \right], \quad (5)$$

where  $\rho_{j\sigma}(\mathbf{r},t) = |\phi_{j\sigma}(\mathbf{r},t)|^2$ .

Equation (4) is an implicit equation for  $V_{x\sigma}^{KLI}$  and can be solved analytically. It requires only the inversion of an  $(n_{\sigma}-1) \times (n_{\sigma}-1)$  matrix,  $n_{\sigma}$  being the number of electrons with spin  $\sigma$ . The main advantage of this scheme is that it leads to a correct asymptotic behavior for the exchange potential. As a consequence, the energy eigenvalue of the highest-occupied Kohn-Sham orbital corresponds to the ionization energy of the system, satisfying Koopman's theorem [24].

One further approximation in our calculation is the restriction for all particles to move in one dimension, along the laser linear polarization. This approximation has been widely used in the case of atoms or molecules strongly interacting with lasers, as it retains the essential physical properties of the systems. In order to remove the singularity for  $x=X_j$ , we will use in Eqs. (2) and (3) the ‘‘soft Coulomb’’ potential [25]

$$V_j(x) = \frac{-Z}{\sqrt{a^2 + (x-X_j)^2}}. \quad (6)$$

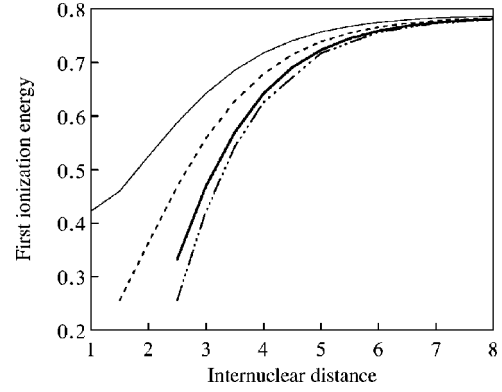


FIG. 1. First ionization energy for a linear chain of ‘‘neon’’ atoms as a function of the internuclear distance  $R$ , for various cluster size:  $N=2$  (thin line),  $N=3$  (dashed line),  $N=5$  (thick line), and  $N=7$  (dot-dashed line). The asymptotic value  $I_p=0.79$  a.u. corresponds to the ionization energy of the isolated atom.

This amounts to replace the electron-nucleus distance  $|\mathbf{r}-\mathbf{R}_j|$  by  $\sqrt{a^2+(x-X_j)^2}$  in Eq. (3) and the electron-electron distance  $|\mathbf{r}-\mathbf{r}'|$  by  $\sqrt{b^2+(x-x')^2}$  in Eqs. (2) and (5). The values of the adjustable parameters  $a$  and  $b$  have to be determined numerically in order to reproduce at best the relevant physical properties for the ‘‘atom’’ considered. As in a one-dimension space the only symmetry is parity, closed shells in a ‘‘rare-gas’’ atom have only two electrons. Each atom is then described as a system with two active electrons evolving in the presence of a ionic core with net charge  $Z=2$ . In the following, we have modeled ‘‘neon’’ atoms, the  $a$  parameter being chosen in order to reproduce the ionization energy of the  $Ne^+$  ion:  $I_{p,Ne^+}=1.50$  a.u.,  $a=0.98$  in Eq. (6). Then,  $a$  being fixed,  $b$  is determined in accordance with the ionization energy of the neutral  $Ne$ :  $I_{p,Ne}=0.79$  a.u.,  $b=1.04$ . Here, the values of  $a$  and  $b$  are accidentally very close to each other and can differ significantly when describing other systems.

The cluster is modeled by a linear chain of atoms, located at regular intervals. In the present study, we consider that the massive nuclei have no time to move significantly from their equilibrium position and, therefore, are kept fixed. This is justified given the short duration of the laser pulses that are considered ( $\tau < 50$  fs) and the moderate ionization of the cluster (see below, Sec. III).

The linear chain is made of equally spaced atoms, located at  $X_{j+1}=X_j+R$ , where  $R$  is the internuclear distance. Typical values for  $R$  are between 6 and 8 a.u., representative of van der Waals clusters. The orbitals  $\phi_{i\sigma}$  are represented on a grid in coordinate space. The initial state is obtained by solving iteratively the time-independent Kohn-Sham equations. The first ionization energy  $I_p$  of the system, corresponding to the value of the highest orbital energy, is illustrated in Fig. 1 as a function of  $R$ , for various numbers  $N$  of atoms in the cluster. Starting from smaller values of  $R$  the ionization energy increases smoothly to its asymptotic value  $I_p=0.79$  a.u., corresponding to the ionization energy of the isolated atom. Note that this behavior, obtained for atomic clusters, in the framework of density-functional theory, is different from the one shown in Ref. [12], for ionized clus-

ters in the single-active electron approximation, where the ionization energy is a decreasing function of the internuclear distance. The present increase of the ionization energy with  $R$  is due to the fact that we are dealing with neutral atoms, producing an efficient screening of the nucleus charge. Moreover, electronic interactions that are included in our model, lead to electronic states well localized on each nucleus.

The propagation in time is done through a unitary Peaceman-Rachford propagator [26]. To avoid reflexion at the grid boundary, we use absorbing boundaries. This implies that in case of atomic ionization, the norm of the orbitals will decrease in time.

The number of emitted electrons from the cluster is defined as

$$\mathcal{N}(t) = \mathcal{N}_0 - \int_{box} dx \rho(x, t), \quad (7)$$

where  $\mathcal{N}_0$  is the number of electrons inside the cluster at time  $t=0$ . To evaluate the effect of the cluster size on the ionization mechanism, it is convenient to define the number of emitted electrons per atom through the relation  $\mathcal{N}_a(t) = \mathcal{N}(t)/N$ . Note that these quantities are only mildly sensitive to the size of the grid. In the framework of the TDDFT, the dipole moment is [23]

$$d(t) = \int_{box} dx x \rho(x, t) \quad (8)$$

and the harmonic yields are obtained from the Fourier transform of the dipole acceleration  $\ddot{d}(t)$ . Again, for the sake of comparison, an average harmonic yield per atom will be defined.

### III. CLUSTER IONIZATION

The laser is supposed to be polarized along the  $x$  direction, with a frequency  $\omega_L$  and a peak amplitude  $E_0$ . The envelop of the electric field is chosen to be trapezoidal, with one-cycle turn-on and turn-off and a 16-cycle flat top. In these conditions, we have calculated the number of emitted electrons per atom  $\mathcal{N}_a$  at the end of the laser pulse as described above, for a frequency  $\omega_L = 1.55$  eV (Ti:Saph laser) and for various laser intensities. One of the key parameter to describe the system is the internuclear distance. Although, in van der Waals clusters, typical values of the equilibrium distance are between 6 a.u. and 8 a.u., it is interesting to analyze the effect of the internuclear distance on ionization in a wider range.  $\mathcal{N}_a$  is displayed in Fig. 2, as a function of  $R$  in the two-atom case. We first note that for the laser intensities presented here, ionization starts to decrease with  $R$ . This is related to the variation of the first ionization energy  $I_p$ , as shown in Fig. 1. For small values of  $R$ , it takes seven photons to ionize the system. As  $I_p$  increases with  $R$ , ionization requires 14 photons when the asymptotic value corresponding to the ionization energy of the isolated atom is reached. However, for larger distances, ionization becomes a non-monotonic function of  $R$ , starting from a small bump for the

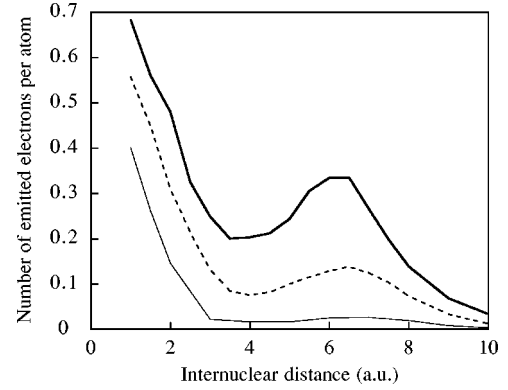


FIG. 2. Number of emitted electrons per atom at the end of the pulse as a function of the internuclear distance for two “neon” atoms. The laser frequency is  $\omega_L = 1.55$  eV and the laser peak intensity is  $I_L = 10^{14}$  W/cm<sup>2</sup> (thin line),  $I_L = 1.5 \times 10^{14}$  W/cm<sup>2</sup> (dashed line), and  $I_L = 2 \times 10^{14}$  W/cm<sup>2</sup> (thick line).

lowest laser intensity  $I_L = 10^{14}$  W/cm<sup>2</sup> to a large enhancement around  $R = 6$  a.u. for higher intensity  $I_L = 1.5 \times 10^{14}$  W/cm<sup>2</sup> and  $I_L = 2 \times 10^{14}$  W/cm<sup>2</sup>. This enhancement has already been predicted in the case of molecular ions [5,6]. This phenomenon, dubbed charge-resonance-enhanced ionization is interpreted in terms of laser-induced localization of the electron in the molecular ion and quasistatic-ionization barrier suppression. A similar behavior has been seen also in  $H_2$ , although not so spectacular than in ions because of the screening due to the other electron, [14,15].

Next, we show in Fig. 3 the number of emitted electrons at the end of the pulse as a function of the internuclear distance  $R$  for a fixed laser intensity  $I_L = 1.5 \times 10^{14}$  W/cm<sup>2</sup> and various  $N$ . Ionization is strongly enhanced but the critical distance, around  $R \approx 4 - 5$  a.u., for which this enhancement appears is smaller than in Fig. 2. On the other hand, we note that this effect increases with the number of atoms in the chain.

Although the results shown here for atomic clusters look similar to the ones obtained with simple molecular systems

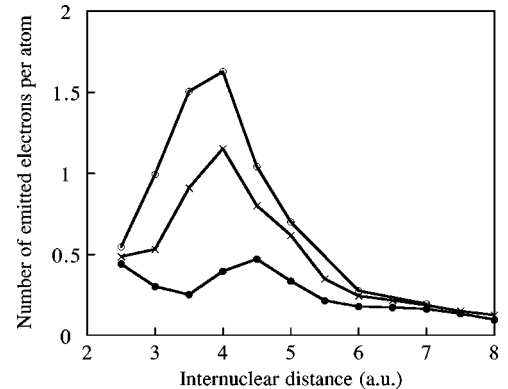


FIG. 3. Number of emitted electrons per atom at the end of the pulse as a function of the internuclear distance for chains of  $N=3$  (●), 5 (×), and 7 (○) “neon” atoms. The laser frequency is  $\omega_L = 1.55$  eV and the laser peak intensity is  $I_L = 1.5 \times 10^{14}$  W/cm<sup>2</sup>.

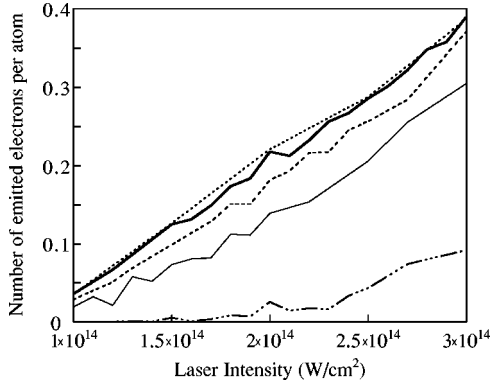


FIG. 4. Number of emitted electrons at the end of the pulse as a function of the laser intensity for the isolated atom (dot-dashed line) and for chains of  $N=2$  (thin line), 3 (dashed line), 5 (thick line), and 7 (dotted line) “neon” atoms. The laser frequency is  $\omega_L = 1.55$  eV and the internuclear distance is  $R=8$  a.u.

$H_2^+$  or  $H_2$ , we would like to stress an important difference. In molecules, the internuclear distance for which the enhancement is observed is larger than the equilibrium distance. It implies that, for long laser pulse, as ionization takes place and the nuclei start to move apart, the critical value may be reached, leading suddenly to higher ionization rates, which then can be followed by the Coulomb explosion of the molecule. In the present case, the typical values for the equilibrium distance of the cluster are roughly between 6 and 8 a.u., which is already larger than the critical distance for  $N \geq 3$ , around  $R \approx 4-5$  a.u. leading then to a different dynamics for ionization.

We turn now to the question of the influence of the laser intensity on the ionization process, keeping fixed the internuclear distance  $R$ . The results are shown in Fig. 4 for an isolated atom and for rows containing from two to seven atoms with an internuclear distance  $R=8$  a.u. Note that this distance, which is typical of van der Waals clusters, does not correspond to the enhancement regime just discussed above. As expected, the number of emitted electrons increases with the laser intensity. However, one can see a very strong increase of ionization with the number of atoms in the cluster, as soon as  $N \geq 2$ , seeming to saturate beyond  $N=5$ . In order to understand this trend, we have computed the electronic charge located around each nuclear site  $X_j$  as following:

$$Q(j,t) = \int_{X_j-d}^{X_j+d} dx \rho(x,t), \quad (9)$$

with  $d=2$  a.u., which amounts to follow in time the electron density within  $\pm 2$  a.u. in the vicinity of each nucleus within the cluster. The results are presented in Fig. 5 for the case of a chain of six atoms. The case of an isolated atom is also indicated for reference. The analysis shows that the atomic ionization rates depend only on the number of neighbors of an atom within the chain. More precisely, the higher ionization rates are observed for atoms with two neighbors. This contrasts with outer atoms that have only one. Indeed, the slope of the curves for the inner sites (dotted line) is approximately twice the slope for the outer ones (thin line), both

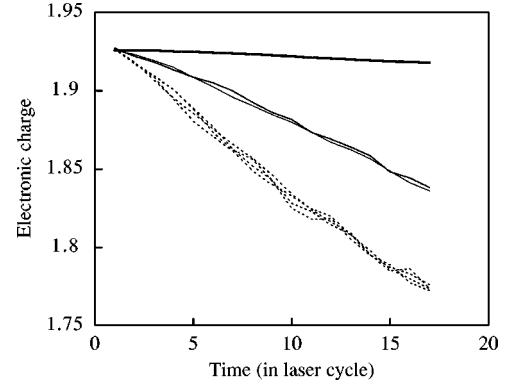


FIG. 5. Electronic charge located around each nucleus within the cluster, defined in Eq. (9), as a function of time for the isolated atom (thick line) and for a chain of  $N=6$  atoms. The solid lines correspond to the outer sites whereas, the dotted lines denote the inner sites. Note that  $Q(j,0) \leq 2$  as we integrate only within  $\pm 2$  a.u. The laser frequency is  $\omega_L = 1.55$  eV, the laser intensity is  $I_L = 1.5 \times 10^{14}$  W/cm<sup>2</sup> and the internuclear distance is  $R=8$  a.u..

being an order of magnitude larger than the slope for the isolated atom (thick line). The reason is that the electric field created by a “charged neighbor” lowers the potential barrier and dramatically eases the ionization process, see for example [17,27]. At inner sites, this is the case twice per cycle, whereas it happens only once per cycle for the outer sites. As the relative weights of the outer sites decrease when  $N$  increases, the average ionization yield shown in Fig. 4 saturates for  $N \geq 5$ .

#### IV. HARMONIC GENERATION

This ionization property of clusters gives already some indication on the possibility to generate high-order harmonics. This is because ionization and harmonic generation are, in some sense, competing processes. As the isolated atoms or small clusters can withstand higher laser intensities without being ionized, they will lead to higher emission rates in the high intensity regime. On the contrary, as a high ionization rate prevents harmonic generation, large clusters can generate harmonics only at lower intensities or for ultrashort pulses.

Let us first recall the semiclassical three-step model, which provides a physical understanding of high-order harmonic generation [28]. In this “simple man’s” theory, the atoms are first ionized by tunneling through the effective barrier. The free electrons then follow a classical trajectory in the presence of the laser, moving back and forth. While they return to the ionic core, the free electrons can recombine into the atomic ground state, emitting the acquired kinetic energy plus the binding energy in the form of an odd harmonic photon. This model predicts photon energies up to the limit  $I_p + 3.2U_p$ , where  $I_p$  is the ionization potential of the atom and  $U_p = I_L / (4\omega_L^2)$  is the ponderomotive energy, [29,28], see also Ref. [30] for a quantum description. The model has been extended to two-center binding potentials for harmonic generation from the molecular ion  $H_2^+$  [8,9]. The analysis of the different trajectories in such a two-center system indicates



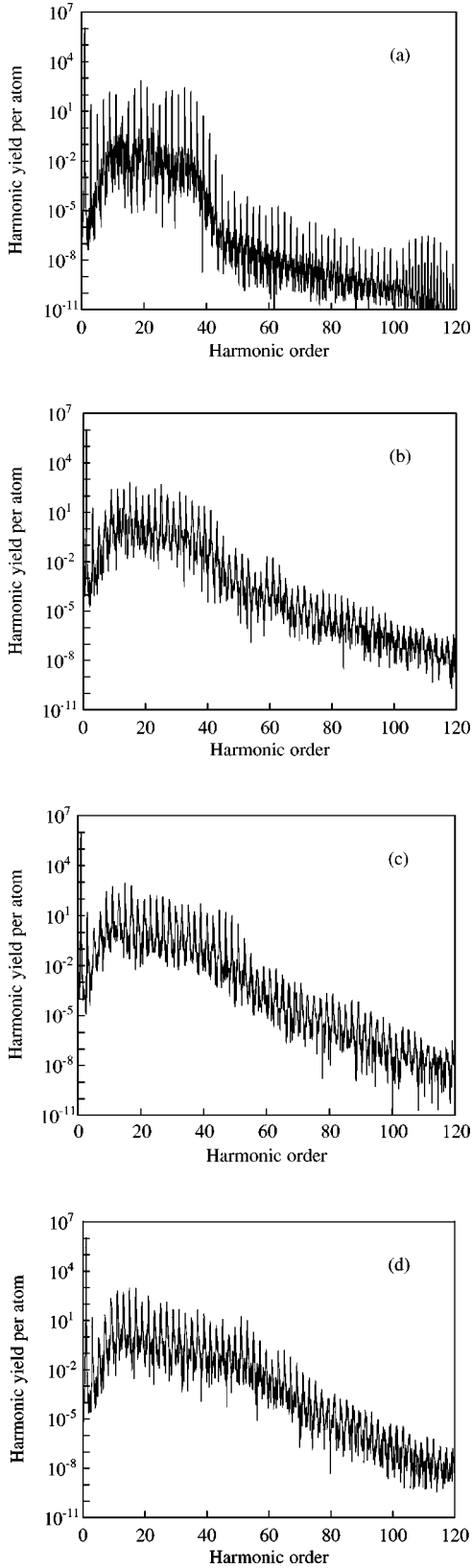


FIG. 6. Harmonic yield per atom  $I_N(\omega)/N^2$  as a function of the harmonic order  $\omega/\omega_L$  for the isolated atom (a) and for chains of  $N=3$  (b), 5 (c), and 7 (d) atoms. The laser frequency is  $\omega_L = 1.55$  eV, the laser intensity is  $I_L = 1.5 \times 10^{14}$  W/cm<sup>2</sup> and the internuclear distance is  $R=8$  a.u..

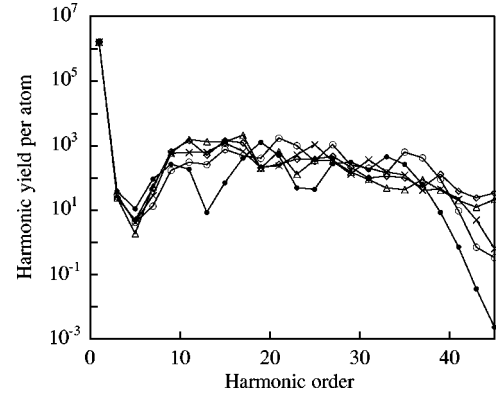


FIG. 7. Harmonic yield per atom  $I_N(\omega)/N^2$  as a function of the harmonic order  $\omega/\omega_L$  in the plateau region for the isolated atom ( $\bullet$ ) and for chains of  $N=2$  ( $\circ$ ), 3 ( $\times$ ), 5 ( $\diamond$ ), and 7 ( $\triangle$ ) atoms. Same conditions as in Fig. 6.

that while the electrons move from one center to the other, a strong harmonic emission can be expected in the plateau region, recombination on the other core leading to photons of much higher energies than those obtained in isolated atoms [10]. However, for the molecular case, the maximum kinetic energy gained by the electrons strongly depends on the distance between the cores. Kinetic energies up to  $8U_p$  can be reached in collisions occurring with the neighboring ion when the internuclear distance is  $R = \pi\alpha_0$ , where  $\alpha_0 = E_0/\omega_L^2$  is the amplitude of the quiver motion of the free electron in the laser field [9]. Note that in the intensity range considered here, this value is huge compared to usual internuclear distance in molecules at equilibrium. It has been shown, however, that in the case of a multiwell structure, the optimal distance can be reached by increasing the size of the system and that photons with energy up to  $I_p + 8U_p$  can be produced [12].

We note that such an analysis has been carried out for molecular systems, where the electronic wave function displays a highly delocalized character, thus, permitting coherent recombination on other nuclear sites. The question is to determine whether a similar process can occur with weakly delocalized systems, such as atomic clusters.

An answer can be deduced from the analysis of harmonic spectra, as derived from the Fourier transform of the time-dependent electronic dipole acceleration of clusters with different size. In a monomer gas, the dependence of the harmonic yield as a function of the number  $N$  of atoms in the sample is the usual quadratic form  $N^2$ . We have compared the ratio  $I_N(\omega_L)/N^2$  for different values of  $N$  to measure the efficiency to generate high-order harmonics of a cluster of  $N$  atoms as compared to  $N$  isolated atoms. Here  $I_N(\omega_L)$  is the intensity generated by the cluster of  $N$  atoms at the frequency  $\omega_L$ . Typical spectra are shown in Fig. 6 for a laser frequency  $\omega_L = 1.55$  eV, an fixed intensity  $I_L = 1.5 \times 10^{14}$  W/cm<sup>2</sup>, and various size of the cluster. For the sake of comparison, we display also in Fig. 7 the harmonic yield per atom below the single atom cutoff at  $\omega_c = I_p + 3.2U_p$ .

The harmonic yield per atom presented in Fig. 7 shows that no significant enhancement can be expected for atomic clusters in this plateau region. The fact that for some har-

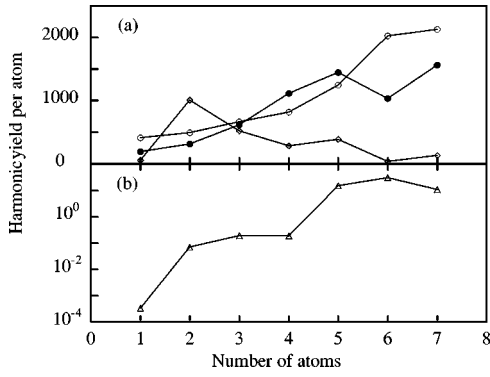


FIG. 8. Harmonic yield  $I_N(\omega)/N^2$  as a function of the number of atoms in the cluster for some representative harmonics in the plateau (a):  $\omega = 11\omega_L$  ( $\bullet$ ),  $\omega = 17\omega_L$  ( $\circ$ ),  $\omega = 29\omega_L$  ( $\diamond$ ), and beyond the cutoff (b)  $\omega = 43\omega_L$  ( $\triangle$ ). Note the change of scale. Same conditions as in Fig. 6.

monics, the emission rate is larger for the cluster than for the isolated atom is more likely due to resonant processes, but no general pattern can be drawn for the harmonic emission, below the cutoff, as a function of the size of the clusters. Typical behaviors are shown in Fig. 8(a) as a function of the number of atoms in the clusters. It appears that some harmonics display a rather growing behavior when  $N$  increases, see for instance harmonics 11 and 17. However, it can be rather “chaotic” for some others (29th harmonic).

More interesting is the behavior of the harmonic emission at higher frequencies, i.e., beyond the cutoff for the single atom. For the isolated atom, the plateau extends up to  $\omega \approx 33\omega_L$ , i.e., in good agreement with the  $I_p + 3.2U_p$  law. Then, one can see that the harmonic yield in the cutoff region increases as soon as  $N \geq 3$ , giving higher values for the position of the cutoff, see Fig. 8(b). Moreover, for the larger clusters, very high-order harmonics appear, even above the classical  $I_p + 8U_p$  limit discussed above.

From these results, it clearly appears that, as in the case of molecules or ionized clusters, recombination on neighboring ions is responsible for high-order harmonic generation in the cutoff region. However, due to the atomic character of the system, leading to an initial strong localization of the electronic wave function on the parent ion, this process is not the dominant one, so that no enhancement in the plateau region is to be expected: it is only visible beyond the cutoff. The appearance of harmonics having an energy greater than  $I_p$

$+8U_p$  has been predicted in the case of an ionized cluster [12]: before recombining with an ion in the chain, electrons can gain kinetic energy during the interaction with the intermediate ions. This process is responsible for the unusual shape of our spectra for larger clusters. The spectrum shown in Fig. 7(d), displaying no clear cutoff but rather a regular decrease, indicates that the electron can acquire much more energy during its classical excursion within the partially ionized cluster.

## V. CONCLUSION

In the present paper, we have presented a model designed to investigate the response of a rare-gas cluster to an intense short laser pulse. The model is based on the time-dependent density-functional theory, designed to incorporate correlation effects due to electron-electron interactions. The cluster has been modeled as a row of atoms aligned along the laser polarization direction. The nuclei are equally spaced and electron-nuclei and electron-electron interaction are modeled with the help of a “soft-Coulomb” potential. The exchange potential has been approximated through the so-called optimized potential method. After solving numerically the time-dependent Kohn-Sham equations, we have compared the ionization yield obtained for the isolated atom and for the clusters. We have shown that van der Waals clusters can exhibit higher ionization yields. We have also presented the harmonic spectra generated by small atomic clusters. In general, it is found that no systematic enhancement is obtained in the plateau region as recombination on the parent ion is the dominant process. However, as in the case of molecules, recombination on neighboring ions can extend the harmonic spectrum to much higher frequencies, beyond the single atom cutoff.

## ACKNOWLEDGMENTS

We gratefully acknowledge useful discussions with Professor E.K.U. Gross. The Laboratoire de Chimie Physique-Matière et Rayonnement is a Unité Mixte de Recherche, Associée au CNRS, UMR 7614, and is Laboratoire de Recherche Correspondant du CEA, LRC No. DSM-98-16. Parts of the computations have been performed at the Center de Calcul pour la Recherche (CCR, Jussieu, Paris) and at the Institut du Développement et des Ressources en Informatique Scientifique (IDRIS).

- 
- [1] T. Ditmire, J.W.G. Tisch, E. Springate, M.B. Mason, N. Hay, J.P. Marangos, and M.H.R. Hutchinson, *Phys. Rev. Lett.* **78**, 2732 (1997).  
 [2] M. Lezius, S. Dobosz, D. Normand, and M. Schmidt, *Phys. Rev. Lett.* **80**, 261 (1998).  
 [3] T.D. Donnelly, T. Ditmire, K. Neuman, M.D. Perry, and R.W. Falcone, *Phys. Rev. Lett.* **76**, 2472 (1996).  
 [4] J.W.G. Tisch, T. Ditmire, D.J. Fraser, N. Hay, M.B. Mason, E. Springate, J.P. Marangos, and M.H.R. Hutchinson, *J. Phys. B* **30**, L709 (1997).  
 [5] T. Seideman, M.Yu Ivanov, and P.B. Corkum, *Phys. Rev. Lett.* **75**, 2819 (1995); D.M. Villeneuve, M.Yu Ivanov, and P.B. Corkum, *Phys. Rev. A* **54**, 736 (1996).  
 [6] T. Zuo and A.D. Bandrauk, *Phys. Rev. A* **52**, R2511 (1995).  
 [7] H. Yu and A.D. Bandrauk, *Phys. Rev. A* **56**, 685 (1997).  
 [8] P. Moreno, L. Plaja, and L. Roso, *Europhys. Lett.* **9**, 629 (1994).  
 [9] A.D. Bandrauk and H. Yu, *J. Phys. B* **31**, 4243 (1998); *Phys. Rev. A* **59**, 539 (1999).  
 [10] R. Kopold, W. Becker, and M. Kleber, *Phys. Rev. A* **58**, 4022

- (1998).
- [11] S.X. Hu and Z.Z. Xu, Phys. Rev. A **56**, 3916 (1997).
- [12] R. Numico, D. Giulietti, A. Giulietti, L.A. Gizzi, and L. Roso, J. Phys. B **33**, 2605 (2000).
- [13] P. Martin, J. Phys. B **29**, L635 (1996).
- [14] H. Yu, T. Zuo, and A.D. Bandrauk, Phys. Rev. A **54**, 3290 (1996); **56**, 685 (1997).
- [15] A. Saenz, Phys. Rev. A **61**, 051402 (2000).
- [16] T. Ditmire, E. Springate, J.W.G. Tisch, Y.L. Shao, M.B. Mason, N. Hay, J.P. Marangos, and M.H.R. Hutchinson, Phys. Rev. A **57**, 369 (1997).
- [17] C. Rose-Petruck, K.C. Schafer, K.R. Wilson, and C.P.J. Barty, Phys. Rev. A **55**, 1182 (1997).
- [18] M. Brewczyk, C.W. Clark, M. Lewenstein, and K. Rzazewski, Phys. Rev. Lett. **80**, 1857 (1998).
- [19] V. Véniard, R. Taïeb, and A. Maquet, Phys. Rev. A **60**, 3952 (1999).
- [20] E. Runge and E.K.U. Gross, Phys. Rev. Lett. **52**, 997 (1984).
- [21] J.B. Krieger, Y. Li, and G.J. Iafrate, Phys. Rev. A **45**, 101 (1992).
- [22] C.A. Ullrich, U.J. Gossmann, and E.K.U. Gross, Phys. Rev. Lett. **74**, 872 (1995).
- [23] C. A. Ullrich, S. Erhard, and E. K. U. Gross, in *Super-intense Laser-Atoms Physics IV*, edited by H. G. Muller and M. V. Fedorov (Kluwer Academic Publishers, Dordrecht, The Netherlands, 1996), p. 267.
- [24] J. Chen, J.B. Krieger, Y. Li, and G.J. Iafrate, Phys. Rev. A **54**, 3939 (1996).
- [25] Q. Su and J.H. Eberly, Phys. Rev. A **44**, 5997 (1991), and references therein.
- [26] K. C. Kulander, K. J. Schafer, and J. L. Krause, in *Atoms in Strong Fields*, edited by M. Gavrilá [Adv. At. Mol. Opt. Phys. Suppl. **1**, 247 (1992)].
- [27] E.M. Snyder, S.A. Buzza, and A.W. Castleman, Phys. Rev. Lett. **77**, 3347 (1996).
- [28] P.B. Corkum, Phys. Rev. Lett. **71**, 1994 (1993).
- [29] J.L. Krause, K.J. Schafer, and K.C. Kulander, Phys. Rev. Lett. **68**, 3535 (1992).
- [30] M. Lewenstein, Ph. Balcou, M.Yu. Ivanov, A. L'Huillier, and P.B. Corkum, Phys. Rev. A **49**, 2117 (1994); W. Becker, S. Long, and J.K. McIver, *ibid.* **50**, 1540 (1994).